CONF-951007--21

Presented at 188th Meeting of the Electrochemical Society, Chicago, Illinois, October 8–13, 1995 and published in *Thin-Film Solid Ionic Devices and Materials*, ed. by J. B. Bates, Electrochemical Society, Pennington, New Jersey.

5-VOLT AND 4.6 V PLATEAUS IN $LiMn_2O_4$ THIN FILMS

J. B. Bates, D. Lubben, N. J. Dudney, R. A. Zuhr
Solid State Division, Oak Ridge National Laboratory
Oak Ridge, TN 37831-6030

and

F. X. Hart
Department of Physics, University of the South, Sewanee, Tennessee 37375

Prepared by
SOLID STATE DIVISION
OAK RIDGE NATIONAL LABORATORY
Managed by
LOCKHEED MARTIN ENERGY RESEARCH CORP.
under
Contract No. DE-AC05-96OR22464
with the
U.S. DEPARTMENT OF ENERGY
Oak Ridge, Tennessee

January 1996

5-Volt and 4.6 V Plateaus in $LiMn_2O_4$ Thin Films

J. B. Bates , D. Lubben, N. J. Dudney, R. A. Zuhr, and F. X. Hart*
Solid State Division, Oak Ridge National Laboratory
P.O. Box 2008, Oak Ridge, Tennessee 37831-6030

ABSTRACT

Additional plateaus with median voltages of ~4.6 V, and ~5 V have been observed on charging thin film lithium batteries with crystalline $LiMn_2O_4$ cathodes to 5.3 V. The total charge extracted from the 4 V and the two additional plateaus corresponded to about $1Li/Mn_2O_4$, but the distribution of capacity among the three plateaus varied from film to film. We speculate that the additional plateaus result from the formation of mixed spinel structures in which a fraction of the 8a sites are occupied by Mn^{2+} or Mn^{4+} ions and a fraction of the Li^+ ions occupy the 16d sites. After charging to 5.3 V, the 4.6 V plateau dissappeared, and the capacity of the 4 V plateau increased at the expense of that of the 5 V plateau. The latter change is attributed to movement of Mn^{3+} or Mn^{5+} ions from 8a to 16d sites.

INTRODUCTION

Recently we reported some results on the characterization of Li-$LiMn_2O_4$ thin-film cells with crystalline spinel cathodes (1,2). Depending on cathode thickness, the cells could sustain current densities of several mA/cm^2 at 25°C and exhibited excellent secondary performance in the 4.5 V to 3.8 V range (4 V plateau). However, the specific capacity of the cathodes in this range varied considerably, from ~30 μAh/mg to ~118 μAh/mg corresponding to x values at the end of charge of 0.7 to 0.2 in $Li_xMn_2O_4$. In view of the recent report (3) of 4.9 V and 4.5 V peaks in the cyclic voltammogram of bulk $LiMn_2O_4$ and since the thin-film amorphous lithium phosphorus oxynitride electrolyte we use is stable from 0 to 5.5 V vs. metallic lithium (4), we were encouraged to charge the cells above 4.5 V to explore the possible existence of high voltage plateaus and possibly to account for the wide variation in capacity of the 4 V plateau. Some results of this investigation were published previously (5).

EXPERIMENTAL PROCEDURES AND RESULTS

The $LiMn_2O_4$ cathodes, ~0.5-μm thick, were deposited over Pt current collectors on alumina substrates by electron beam evaporation and by rf magnetron sputtering (6) of $LiMn_2O_4$. Films deposited by these two techniques are denoted by (eb) and (sp), respectively. The as-deposited amorphous films were annealed at 300–800°C in flowing O_2 for 20 min to 4 h. The heating and cooling rates of the tube furnace were ~20°C/min

---

* Department of Physics, University of the South, Sewanee, Tennessee, 37375

and 10°C/min, respectively. After annealing, X-ray diffraction (XRD) measurements were made over the 2Θ range from 15 to 70°; examples of diffraction patterns for two films are shown in Fig. 1. The labeled peaks originate from the $LiMn_2O_4$ films with the cubic spinel structure, and all other peaks could be assigned to either the alumina substrate or the Pt contact. In a few cases, weak diffraction peaks were observed that were not due to a cubic structure.

Rutherford backscattering measurements were made on four films deposited onto Si substrates before and after annealing at 700°C. While the O/Mn atomic ratios were less than 2 in the as deposited films, the ratios were equal to 2 (±.08) for all four films after annealing.

The thin-film cells were completed by deposition of the electrolyte and lithium anode (2). Constant current charge-discharge curves were obtained using calibrated[a] 1 μA, 10 V test channels of a Maccor battery test system and the following procedure (see Fig. 2): as-fabricated cells were charged from their initial open circuit voltage (OCV), typically ~2.9 V, to 4.5 V at 10 to 20 $\mu A/cm^2$ and held at this potential until the current decreased to 1 μA. The cells were later discharged to 1.5 V and then recharged to 5.3 V at current densities of 2 to 5 $\mu A/cm^2$. The voltage was held fixed at 5.3 V until the current decreased below 1 μA before beginning the next discharge. In a few cases, open circuit voltage curves were obtained before and after charging to 5.3 V: charge was inserted (removed) in successive 2 μAh steps after the voltage change was <5 mV/h. All cells were cycled between 4.5 V and 3.8 V at different current densities before and after charging to 5.3 V.

A combined set of charge and discharge curves between 5.3 V and 1.5 V plotted as V vs. x for (eb)$Li_xMn_2O_4$ is shown in Fig. 2. The arrows indicate the discharge and charge steps, and the dashed vertical lines divide the curves into three regions associated with three voltage "plateaus" having capacities of Q_1, Q_2, and Q_3. In converting the measured charge in μAh to x in $Li_xMn_2O_4$ it was assumed that x = 1 at the sharp transition from the 4 V to the 2.8 V plateau. The measured charge at this transition, 23 μAh ($Q_1 + Q_2$ in Table I), is close to the charge equivalent to 1 Li, 22 μAh, based on the cathode mass of 0.15 mg calculated from the measured area and thickness and an assumed density of 4.3 g/cm^3. The appearance of the 2.8 V plateau at x > 1 on the discharge curve marks the onset of the two phase regime consisting of the cubic spinel and tetragonal structures (7,8). As the Li concentration increases, there is a second sharp decrease to a 2.1 V plateau which does not appear in the OCV curve. The time for the voltage to relax from 2.1 V to 2.8 V after each 2 μAh increment increased from minutes to hours until x ~ 2. On the charge cycle from 1.5 V, the transition to the stable 2.8 V plateau was also sharp, as shown on the figure. Since the relaxation was fast at either extreme, the charge between the two sharp transitions, Q_3, accurately measures the capacity in the two phase region. As lithium is removed, a sharp increase in voltage to 3.8 V occurs, and the relaxation time increases from minutes to hours as the charge progresses. As x decreases to 1, the relaxation again becomes rapid.

Charge-discharge curves for two (eb) films of similar mass grown under nominally the same conditions in different runs and annealed at 800°C for 60 min are shown in Fig. 3. Values of the charges Q_1, Q_2, and Q_3 and the ratios, $Q_2/(Q_1 + Q_2)$ and $(Q_1 + Q_2)/Q_3$, for

---

[a] Calibrated with a Keithley 617 electrometer with charge and discharge currents from 1 to 100 μA.

these and other films investigated to date are listed in Table I. For films grown in the same run, the data show that increasing the annealing temperature from 400°C to 800°C significantly increased Q_2 at the expense of Q_1 (films U97). For the film with the larger Q_2, an inflection can be observed near the midpoint of the 4 V plateau, indicative of a transition from one cubic phase to another as observed in bulk material (8), whereas no inflection was observed for the film with the smaller Q_2. The presence of two plateaus in the Q_2 region of U97 can be seen more clearly as two peaks in the graph of -dq/dV vs. V shown in Fig. 4; a single broad, asymmetric (-dq/dV) peak in the Q_2 region was observed for U94. We have observed that the presence of a phase transition between 4.5 V and 3.8 V is always associated with larger values of Q_2: $Q_2/(Q_1 + Q_2) > 0.5$.

For two of the cells investigated, an additional voltage plateau at about 4.6 V was observed on the first charge to 5.3 V as shown in Fig. 5. The flat profile observed for this plateau strongly suggests that it is due to the presence of two phases. The capacity of the 4.6 V plateau is about 43% of the total above 3.8 V ($Q_1 + Q_2$) for the sputter deposited film and about 17% for the (eb) film. For these cells, the capacity between 4.5 V and 3.8 V (Q_2) was the smallest fraction of $Q_1 + Q_2$ of all of the films, 20% (Table I).

Table I

Capacities in the 5 V (and 4.5 V), 4 V, and 3V Plateaus of Crystalline $LiMn_2O_4$ Thin Films

Cathode	Capacity (μAh)			Ratios	
	Q_1	Q_2	Q_3	$Q_2/(Q_1 + Q_2)$	$(Q_1 + Q_2)/Q_3$
76D (800°C)	13.1	9.9	22.7	0.4	1.0
U94-3 (700°C)	6.3	5.8	17.4	0.5	0.7
U94-4 (800°C)	7.9	5.4	14.0	0.4	1.0
U97-2 (400°C)	6.3	8.8	19.0	0.4	0.8
U97-3 (500°C)	6.6	9.2	16.9	0.6	0.8
U97-4 (800°C)	3.3	11.8	16.7	0.8	0.9
107D (700°C)	3.6	6.7	12.9	0.6	0.8
115D (800°C)	9.3	13.3	25.2	0.6	0.9
U98 (700°C)*	12.0	3.1	14.6	0.2	1.0
254B (sp, 700°C)*	33.6	8.5	36.4	0.2	1.2

*Capacity of the 4.6 V plateau included in Q_1.

Cycles following the first charge to 5.3 V indicate that a distinct change has occurred in the cathode. The second charge to 5.3 V in Fig. 5b shows that while there remains some capacity above 5 V, the 4.6 V plateau virtually disappears. This is illustrated more clearly by the comparison in Fig.6 of -dq/dV vs. V for the 1st and 2nd charge cycles from 1.5 to 5.3 V of cell 254B. In addition, the capacity upon discharge of the cells between 4.5 V and 3.8 V increased by as much as 80 % following the charge to 5.3 V. In Fig. 2 the increase in Q_2 can be judged by comparing the charge between the short vertical bars on the discharge curves, which mark the 4.5 V and 3.8 V region, with the initial Q_2 region. This can be seen more clearly in Fig. 7 where the "after" discharge curve in this figure was measured following several cycles to 5.3 V. Likewise the later discharge curves in Fig. 5 show the increased capacity of the 4.5 to 3.8 V region for these cells compared with the initial values of Q_2 given in Table I.

DISCUSSION

The charge cycled between 4.5 V and 3.8 V (Q_2) is attributed to Li^+ ions occupying the 8a tetrahedral sites in the spinel lattice, in accordance with all of the prior studies (3,7-8) of bulk $LiMn_2O_4$. As Li^+ is removed from the 8a sites on charging from 3.8 to 4.5 V, Mn^{3+} on the 16d sites are oxidized to Mn^{4+}. Because the charge curves in the Q_1 region of the two cells of Fig. 3 are not flat, we believe that the extraction of Li^+ at ~5 V takes place by a single phase process.

Following one of the arguments advanced by Tarascon et al. (3) for the possible origin of the 4.9 V voltammogram peak observed in bulk $LiMn_2O_4$, we have speculated (3) that the charge Q_1 can be attributed to Li^+ ions located on the 16d octahedral sites of a mixed spinel structure. In the mixed structure, some of the Li^+ ions occupy the 16d sites while some of the Mn ions occupy 8a tetrahedral sites (3):

$$(Li_xMn_{1-x})_{8a}[Li_{1-x}Mn_u^{4+}Mn_v^{3+}X_w]_{16d}. \qquad (1)$$

In Eq. (1), X represents a vacant site, and $u + v + w = 1 + x$. In this model, we assume that the valence of Mn on the 8a sites is either 2+ or 4+, since Mn^{3+} and Mn^{5+} are unlikely to occupy four-coordinate sites (9, 10). When all of the Li^+ ions on the 8a sites have been removed yielding a capacity Q_2, the Li^+ ions on the 16d sites are extracted yielding a capacity Q_1 as the manganese ions on the 8a sites are oxidized: Mn^{2+} to Mn^{3+} or Mn^{4+} to Mn^{5+}. To consider a specific example, for cell U94, the composition from Table I implies that $x = 0.4$ in Eq. 1. Assuming that the fraction of Mn^{3+} is at least equal to the fraction of Li^+ ions on the 8a sites (as required by the observed value of Q_2), then with Mn^{4+} on 8a, the composition is given by $(Li_{0.4}Mn_{0.6}^{4+})[Li_{0.6}Mn_{0.85}^{4+}Mn_{0.4}^{3+}X_{0.15}]O_4$. Alternatively assuming Mn^{2+} on 8a requires a charge balance of 1.15 Mn^{4+}, but u cannot exceed 1.0 if $v = 0.4$ in Eq. 1. If this model is valid, then 0.15 Mn^{4+} ions must occupy some other site, possibly 16c.

During or after the first charge to 5.3 V, we speculate that the Mn^{5+} or Mn^{3+} ions formed on the 8a sites migrate to the 16d sites vacated by the Li^+ ions, in keeping with their preferred six-fold coordination (9,10). On the subsequent discharge, there are fewer 16d sites and more 8a sites available for the Li^+ ions, so that the capacity Q_2 is increased at the expense of Q_1 as observed (Figs. 2, 5, and 7).

While the simple mixed spinel model provides a plausible explanation for the 5 V plateau, we are unable at this time to offer an explanation for the origin of the 4.6 V plateau. Because it is flat, it is clear that this plateau is associated with a two phase region, analogous to the 2.8 V plateau (Fig. 2) in which the lattice transforms from cubic spinel to a tetragonal structure as lithium insertion proceeds beyond x=1 in $Li_xMn_2O_4$. From the curves in Fig. 5, it appears that the capacity originally present at 4.6 V is redistributed mainly to increase the capacity between 3.8 V and 3 V. In spite of the redistribution that occurs, charging to 5.3 V is not a practical means of increasing the capacity of $LiMn_2O_4$ thin films below 4.5 V. Because the resulting irreversible structural damage to the cathode significantly lowers the lithium ion mobility and increases cell resistance, the capacity loss at useful current densities from the increased cell iR is larger than the capacity gained from the redistribution.

The model for the 5 V plateau described above relies on the formation of a mixed spinel. The relative population of Mn ions on octahedral and tetrahedral, i.e. the extent of mixing can, in principle, be determined by comparing the relative intensities of the (111) and (311) Bragg peaks (3): a higher (311)/(111) ratio implies more extensive mixing. Consistent with one of their models, Tarascon et. al. (3) found that the bulk sample with the largest 4.9 V voltammogram peak had the largest (311)/(111) ratio. It appears in the x-ray spectra in Fig. 1 that the (311)/(111) ratio of film U94 is larger that that of film U97 consistent with its larger Q_1/Q_2 ratio (Fig. 2). In general, higher ratios were observed in the x-ray spectra of films with more capacity in the 5 V plateau. However, we know from rocking curve measurements that there is some degree of preferred orientation in the films, so any comparisons of relative peak intensites should be viewed with caution.

The lattice constants on the other hand are not sensitive to orientation. Thackeray and colleagues have observed (11) that defect lithium manganese oxide spinels in which Li^+ ions replace a fraction of the Mn ions on the 16d sites have smaller lattice constants than the stoichiometric material. Additionally, it has been observed in other spinel systems that the lattice constant decreases with increased mixing (12). The interplanar spacings in Fig. 1 determined from the measured peak positions matched exactly, within experimental resolution, the values calculated for a cubic material with the lattice constants of 8.19 Å (film U97) and 8.16 Å (film U94). The smaller ratio $Q_2/(Q_1 + Q_2)$ for U94 compared to U97 is consistent with the smaller lattice constant of the former if indeed the cell constant decreases with increased mixing. As shown in Fig. 8, there is a general trend of decreasing capacity Q_2 with decreasing lattice constant in $LiMn_2O_4$ thin films. However, it does not appear that the thin film results are consistent with those of Tarascon et. al. for bulk $LiMn_2O_4$, as they report (3) a cell parameter of about 8.25 Å for the material that exhibited the largest 4.9 V voltammogram peak.

CONCLUSIONS

In spite of using the same target material, film growth conditions, and post deposition annealing conditions, we have observed a wide variation in capacity of the 4 V plateau in $LiMn_2O_4$ thin films. The remaining lithium, corresponding to a total of $1Li/Mn_2O_4$, was found in a 5 V plateau and, in some cases, a 4.6 V plateau on the first charge to 5.3 V. While higher annealing temperatures (300–900°C) result in higher 4 V capacities in films deposited in the same run, the large run-to-run variation means that a yet unidentified process that occurs during evaporation or sputtering is largely responsible for the

distribution of capacity among the three plateaus. The formation of mixed spinel structures having Mn^{2+} or Mn^{4+} on the 8a sites, with variation in the degree of mixing from run to run, provides a plausible explanation for the distribution of capacity between the 4 V and 5 V plateaus; the (311)/(111) x-ray peak intensities were qualitatively consistent with this model. We offer no explanation for the 4.6 V plateau except to note that it is clearly due to a two-phase process and that weak x-ray peaks associated with a non-cubic structure were observed in the films exhibiting a 4.6 V plateau.

As implied by Eq. (1), a possible cause of the mixing and consequent capacity variation could be deviations in stoichiometry which, in most cases, are too small to be detected from measurements of the O/Mn ratio using RBS. One goal of future research is to obtain analytical data of sufficient accuracy to be able to correlate electrochemical properties with film stoichiometry. As a part of this research, in situ x-ray diffraction and XPS measurements will be used to determine the distribution of manganese ions and their valence states at different stages of the initial charge to 5.3 V and the subsequent cycles.

ACKNOWLEDGEMENTS

This research originated from the suggestion by Professor T. Ohzuku that we charge our thin film cells above 5 V. We also thank Chris Luck for fabricating the thin film cells and Dr. Michael Thackeray and Dr. Jeffery Dahn for helpful discussions and suggestions during the course of this work. We greatfully acknowledge the financial support provided by the Division of Materials Sciences and the Division of Chemical Sciences, U.S. Department of Energy, under contract No. DE-AC05-96OR22464 with Lockheed Martin Energy Research Corp.

REFERENCES

1. J. B. Bates, D. Lubben, and N. J. Dudney, Aerospace and Electronic Systems Magazine, 10, 30 (1995).
2. J. B. Bates, N. J. Dudney, D. L. Lubben, G. R. Gruzalski, B. S. Kwak, Xiaohua Yu, and R. A. Zuhr, J. Power Sources 54, 58 (1995).
3. J. M. Tarascon, W. R. McKinnon, F. Coowar, T. N. Bowmer, G. Amatucci, and D. Guyomard, J. Electrochem. Soc. 141, 1421 (1994).
4. X. Yu, J. B. Bates, and G. E. Jellison, these proceedings.
5. J. B. Bates, D. Lubben, N. J. Dudney, and F. X. Hart, J. Electrochem. Soc. 142, L149 (1995).
6. N. J. Dudney, J. B. Bates, D. Lubben, and F. X. Hart, these proceedings.
7. M. M. Thackeray, W. I. F. David, P. G. Bruce, and J. B. Goodenough, Mat. Res. Bull. 18, 461 (1983).
8. T. Ohzuku, M. Kitagawa, and T. Hirai, J. Electrochem. Soc. 137, 769 (1990).
9. J. B. Goodenough and A. L. Loeb, Phys. Rev. 98, 391 (1955).
10. R. D. Shannon, Acta Cryst. A32, 751 (1976).
11. P. B. Boucher, R. Buhl, and M. Perrin, Acta Cryst. B25, 2326 (1969).

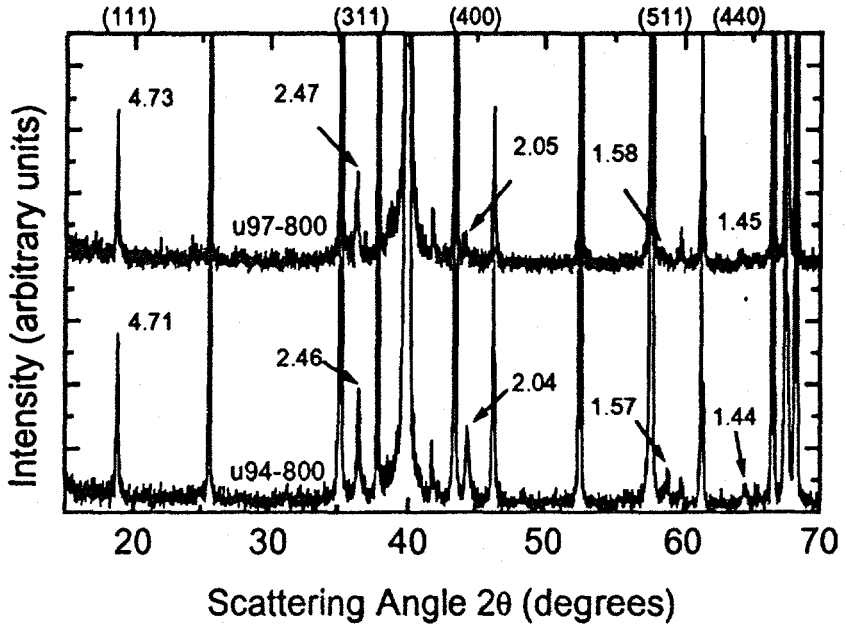

Fig. 1. X-ray diffraction patterns for two films grown in different runs after annealing at in O_2 at 800°C for 1h.

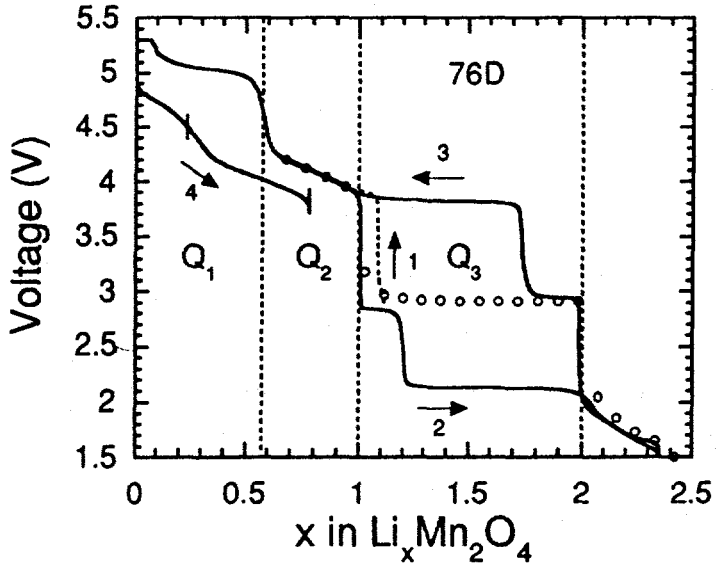

Fig. 2.Combined set of discharge and charge data for cell 76D with an 0.3-μm-thick $LiMn_2O_4$ cathode film annealed at 800°C in O_2 for 20 min. The numbered arrows indicate the order of events: 1- initial charge from 2.9 V to 4.5 V-hold until $i_c \leq 1\mu A$; 2- discharge to 1.5 V; 3- charge from 1.5 V to 5.3 V-hold until $i_c \leq 1\ \mu A$; 4- discharge to 3.8 V. The OCV data shown as the open points were measured between steps 2 and 3.

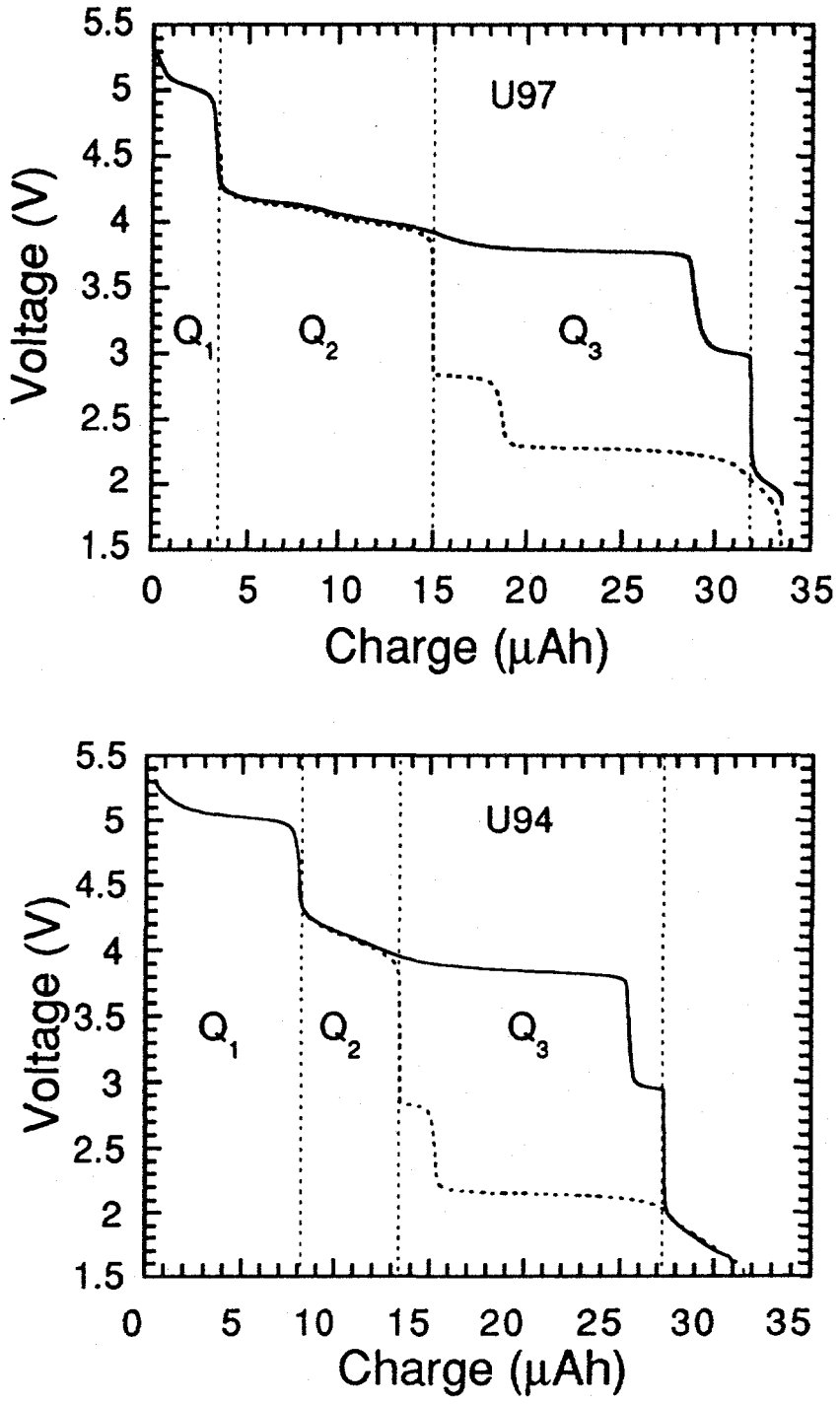

Fig. 3. Discharge-charge curves for ~0.5-μm-thick $LiMn_2O_4$ films grown at different times and annealed at 800°C for 60 min. Dashed line: discharge from 4.5 V to 1.5 V; solid line: charge to 5.3 V and hold until $i_c \leq 1\mu A$.

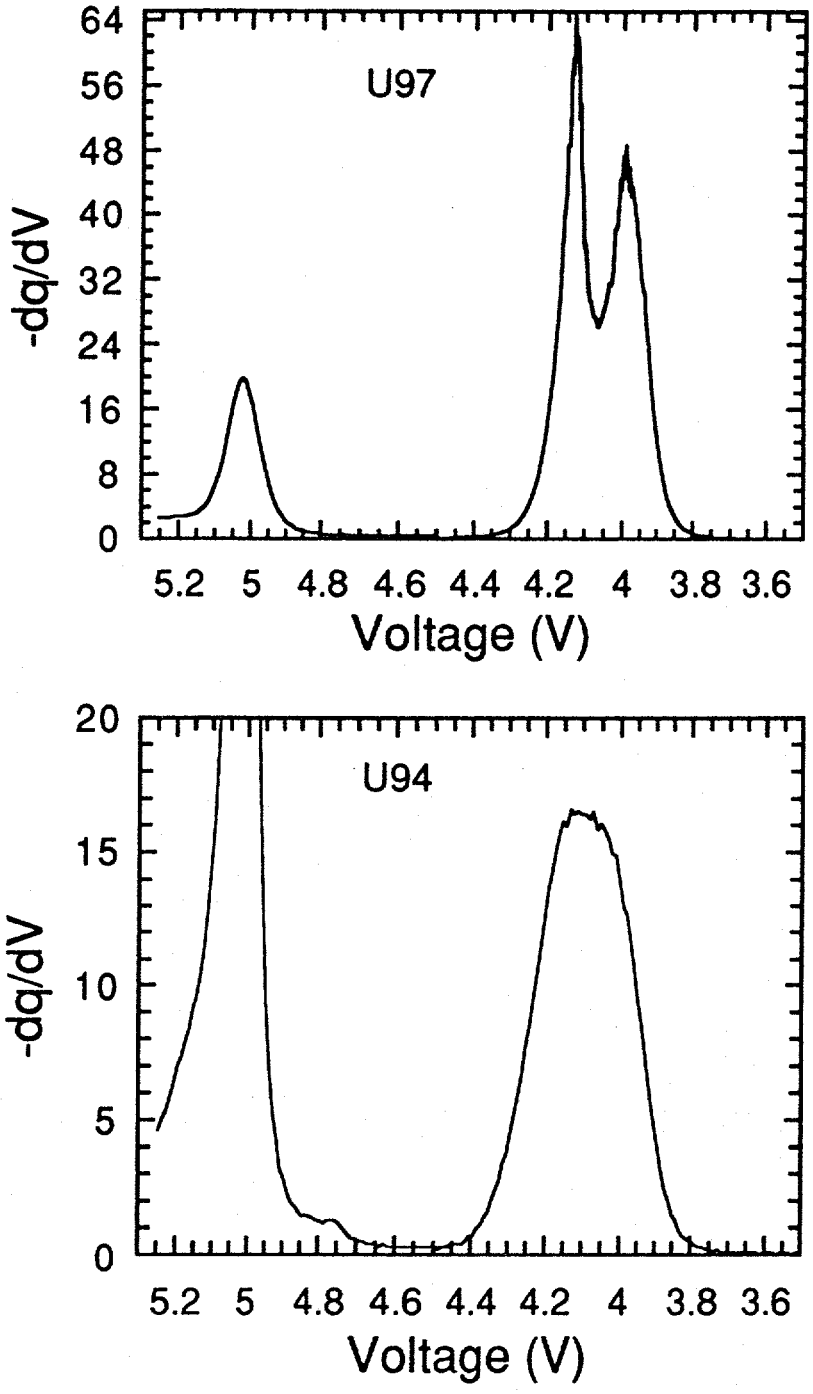

Fig. 4. Composite graphs of -dq/dV vs. voltage for a discharge from 4.5 V to 3.5 V and the 1st charge from 4.5 V to 5.3 V of the two cells of Fig. 3.

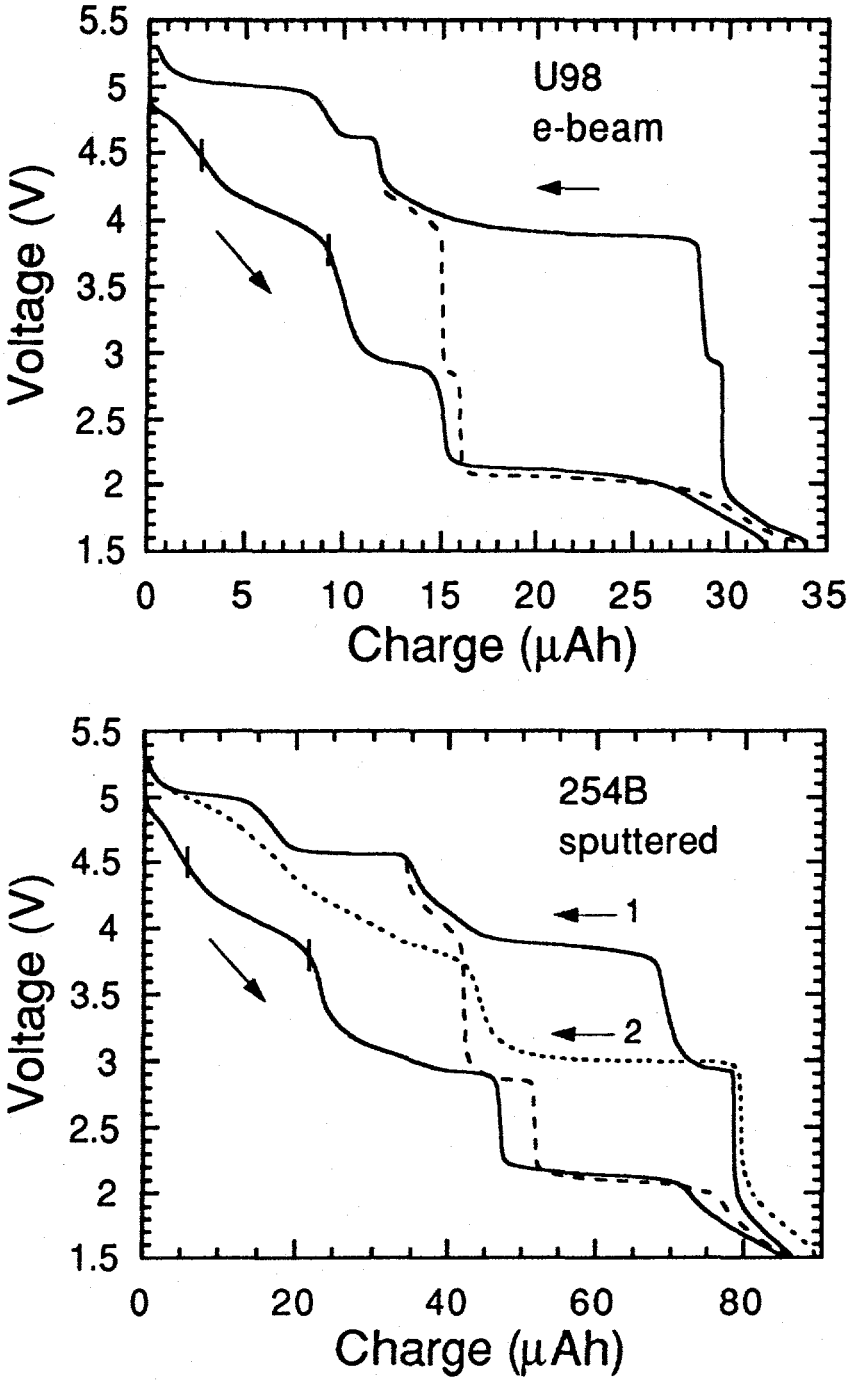

Fig. 5. Discharge from 4.5 V to 1.5 V (coarse dashed line) followed by charge to 5.3 V and discharge to 1.5 V of two cells exhibiting a plateau at 4.6 V. Cathode U98 deposited by electron beam evaporation; cathode 254B deposited by rf magnetron sputtering. Both films annealed in O_2 at 700°C for 1h. The short vertical bars mark the discharge curves at 4.5 V and 3.8 V. The arrows marked by 1 and 2 indicate the 1st and 2nd charge to 5.3 V for cell 254B.

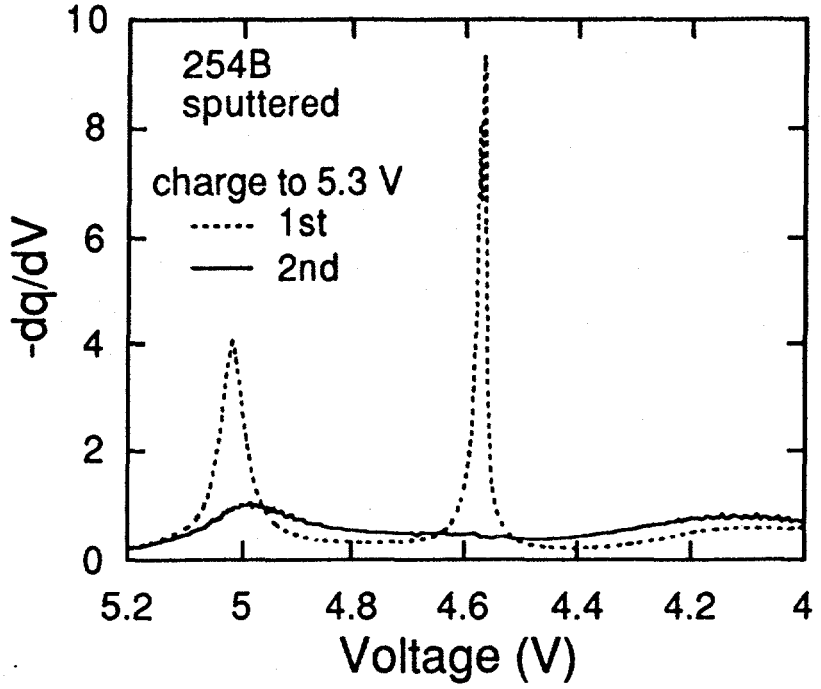

Fig. 6. Comparison of -dq/dV vs. V for the initial and 2nd charge to 5.3 V of cell 254B.

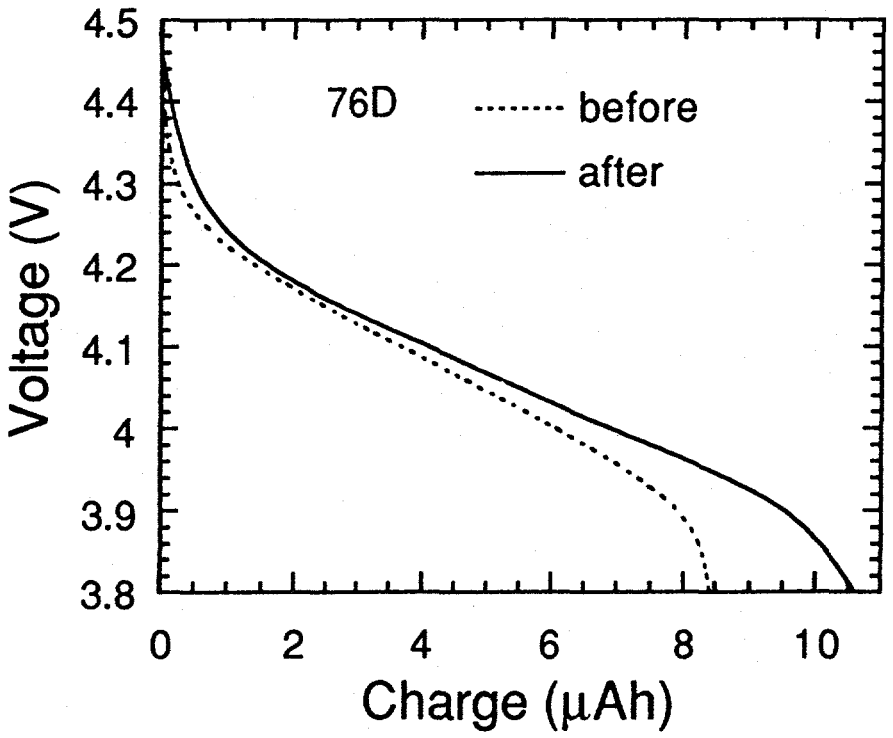

Fig. 7. Discharge curves for cell 76D (Fig. 2) before and after charging to 5.3 V.

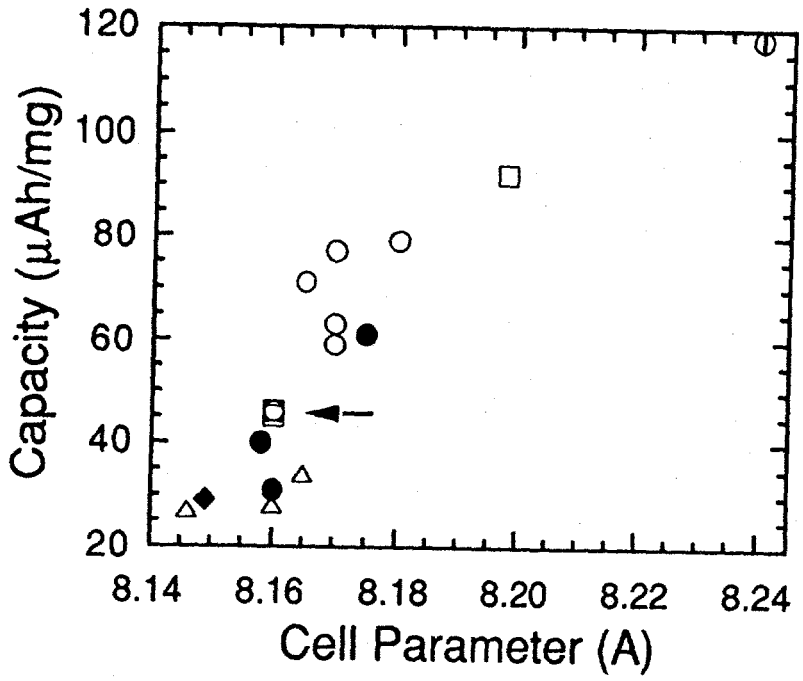

Fig. 8. Specific capacity between 4.5 V and 3.8 V vs. lattice constant . Solid diamond-cathode film deposited by sputtering. All other films deposited by e-beam evaporation. Three data points overlap at position indicated by arrow.